NANO LETTERS

2008
Vol. 8, No. 12
4454-4458

Flexible Carbon Nanotube−Polymer Composite Films with High Conductivity and Superhydrophobicity Made by Solution Process

Chan Luo,[†,‡] Xiaolei Zuo,[‡] Lei Wang,[†] Ergang Wang,[†] Shiping Song,[‡] Jing Wang,[‡] Jian Wang,[*,†] Chunhai Fan,[*,‡] and Yong Cao[†]

Institute of Polymer Optoelectronic Materials and Devices, South China University of Technology, Key Laboratory of Specially Functional Materials, Ministry of Education, Guangzhou 510640, P.R. China, Shanghai Institute of Applied Physics, Chinese Academy of Sciences, Shanghai 201800, P.R. China

Received August 7, 2008; Revised Manuscript Received September 18, 2008

ABSTRACT

CNT/Nafion nanocomposite film made by solution process exhibits high conductivity and superhydrophobicity. The highest water contact angle reaches 165.3 ± 1.9°. The wettability of the film can be controlled by simply varying the filtering rate and the content ratio of Nafion to CNT. We also develop a novel optical method to directly observe the air−solid−liquid interface for the first time. The extraordinary mechanical strength provided by the polymer helps the film retain its conductivity and superhydrobicity after 1000 bending cycles.

Researches and developments of carbon nanotubes (CNTs) toward realistic applications have evolved from investigations of microscopic individual nanotubes to investigations of macroscopic articles.[1] A free-standing carbon nanotube film or sheet assembled by huge numbers of nanotubes has been realized using various techniques such as chemical vapor deposition (CVD),[2] dry-state spinning,[3] and vacuum filtering.[4] The film demonstrated unique optical, electronic, and mechanical properties that make it potentially suitable in the applications of compliant interconnect structures,[2] light-emitting diodes,[3,5] nanotube based field-effect transistors,[4] and dye-sensitized solar cells.[6] However, the weak intermolecular attractions (van der Waals forces) between these submillimeter-long nanotubes may prevent them from long-time operation in practical applications where bending and twisting more or less take place. To overcome such obstacles, carbon nanotube based nanocomposites have emerged as the most promising materials and have been forecasted as "the next generation of composite materials".[7] The composites, typically carbon nanotubes filled with a polymer, not only retain the features of carbon nanotubes such as good electrical and thermal conductivity but also provide the highly desirable mechanical properties of the polymers. Herein, we report a new flexible multifunctional CNT/polymer composite film with superhydrophobicity and high conductivity fabricated by one-step vacuum filtering of CNT-Nafion mixture solution. To investigate the superhydrophobicity, we have successfully developed a novel and simple method to directly observe the air−solid−liquid three-phase interface. We further demonstrate this flexible conductive superhydrophobic film can be implemented as an electrode for biosensors.

Early studies have mostly focused on the superhydrophobic aligned CNT films.[8−11] One problem of such films is that, due to high surface energy of CNT surface, water droplets on aligned CNT films are not stable for prolonged time and will eventually infiltrate into the CNT forest voids.[8] To solve the problem, low surface energy polymers have been successfully coated with aligned CNT films.[8,9] Although the superhydrophobicity is achieved with polymer coatings, it is rarely reported that these films simultaneously show high conductivity because the surface conductivity could be attenuated by the insulated coatings, thus restricting their applications as electrode materials and interconnected conductors. Moreover, polymer coatings function as coverings to modify the CNT film surface rather than fillers to disperse into nanotubes to provide the CNT films with sufficient mechanical strength and flexibility.[7,12] Another big challenge facing the nanotube composites is how to effectively disperse the poorly soluble nanotubes into the polymer matrix.[7]

* To whom correspondence should be addressed. E-mail: jianwang@scut.edu.cn (J.W.); fchh@sinap.ac.cn (C.F.).

† Institute of Polymer Optoelectronic Materials and Devices, South China University of Technology, Key Laboratory of Specially Functional Materials, Ministry of Education.

‡ Shanghai Institute of Applied Physics, Chinese Academy of Sciences.

10.1021/nl802411d CCC: $40.75
Published on Web 11/05/2008

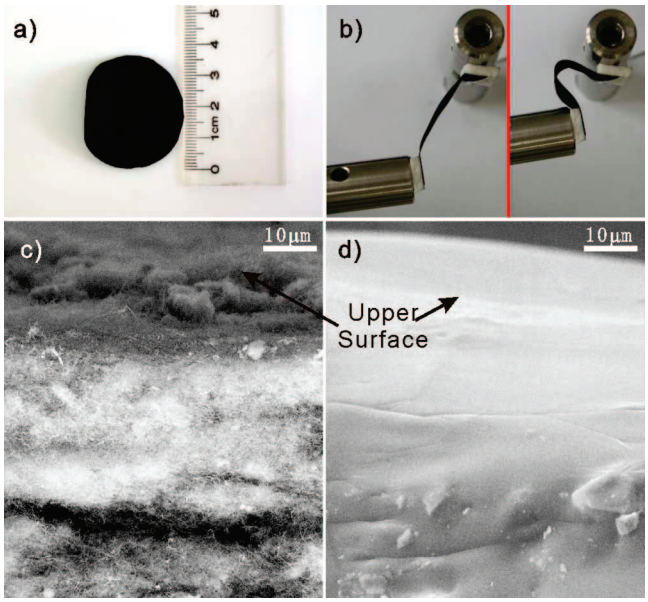

Figure 1. (a) A free-standing CNT/Nafion nanocomposite film (Φ = 36 mm) peeled from the filtration membrane. (b) A piece of nanocomposite film (3 cm × 1 cm) under fatigue test (left: relaxation state; right: bending state). SEM images of the cross-sections of (c) the pure CNT film, and (d) the nanocomposite film heavily mixed with Nafion.

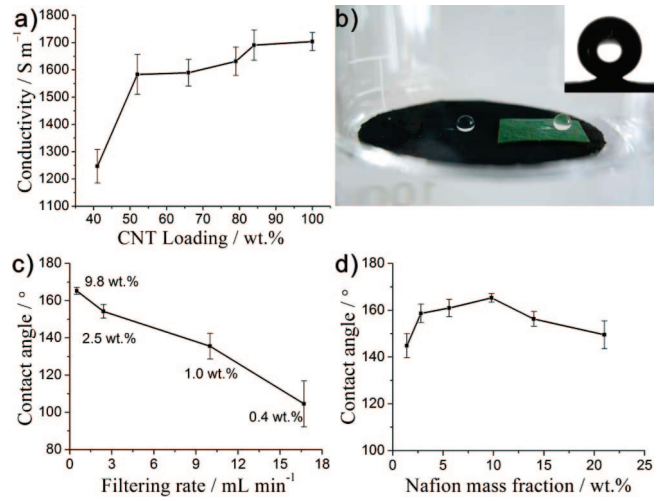

Figure 2. (a) The dependence of electrical conductivities on the CNT loading levels. (b) Two water droplets (10 μL): one is on top of flexible CNT/Nafion nanocomposite film, while the other is on a piece of green fresh lotus leaf. The entire CNNF is floating on the surface of water in a flask. The inset shows a water droplet (1 μL) on the CNNF with a contact angle of 165.3 ± 1.9°. (c) The dependence of the water contact angle on the vacuum filtering rate with the mass fraction indicating the Nafion content ratio in the respective CNNFs. (d) The CA versus the mass fraction of Nafion in the CNNFs.

Indeed, few studies have achieved composites with high CNT volume/weight fractions. Recently, Wang et al. discovered the ability of the perfluorosulfonated polymer Nafion to solubilize both single-walled and multiwalled CNTs (SWNT and MWNT) by simply adding Nafion into alcoholic solutions of CNT. The resulting blends were served as thin layer coatings to modify the electrodes for preparation of oxidase-based amperometric biosensors.[13] The good compatibility and strong interactions between Nafion and CNTs make Nafion more convenient and suitable as a filler to forcefully combine with the nanotubes to fabricate large-area CNT nanocomposite films than previously used polymer fillers, such as epoxy, nylon, styrene butadiene rubber, poly(methyl methacrylate), and polyethylene.[14−18] The one-step vacuum filtration process (described in Supporting Information) employed in the fabrication of CNT/Nafion nanocomposite films (CNNFs) is a facile and low-cost solution process that does not require ultrahigh vacuum. It readily allows CNTs to be intimately mixed with Nafion to form homogeneous nanocomposite films with high CNT volume/weight fractions, which can be effortlessly peeled from the filtration membrane without any visible pinholes or cracks. In addition, using commercially available raw materials makes it possible to fabricate large area films at very low cost.

The free-standing CNNF shown in Figure 1a, typically 50 μm thick, exhibits strong flexibility. In the fatigue test as demonstrated in Figure 1b, the CNNF fabricated by an optimized process has endured 1000 bending cycles without causing any rupture or losing its conductivity and superhydrophobicity. Prior to the fatigue test, its electrical conductivity was measured to be 1690 S m^{-1} by four-point probe method, very close to the conductivity of 1700 S m^{-1} for pure nanotube control films. Its water contact angle was about 155.7°. After the fatigue test, the conductivity slightly decreased to 1620 S m^{-1} and the contact angle became 153.3°. The results demonstrate the superior mechanical properties of the CNNFs provided by the polymer filler. Parts c and d of Figure 1 depict the high-magnification scanning electron microscopy (SEM) images of cross-section of the pure CNT film and CNNF, respectively. The pure CNT film consists of loosely packed multiwall CNTs. On the film, a strip of micrometer-sized crack is clearly observed (Figure 1c). By contrast, the film heavily mixed with Nafion is solid and appears to be entirely filled with the polymer (Figure 1d). The saturated filling reflects the intimate contacts between nanotubes and polymer chains, thereby resulting in the mechanically reinforced nanocomposite films.[7]

The conductivity measurements on the composite films were carried out as a function of CNT loading levels. As shown in Figure 2a, the conductivity of the films saw minimal decline from 100 wt % CNT (pure CNT film) to 52 wt % CNT. The conductivity values remain above 1500 S m^{-1}. However, as the CNT loading level is lowered to 41 wt % CNT, the conductivity of the film suddenly drops to 1250 S m^{-1}. This abrupt change in the conductivity indicates the clear observation of a percolation threshold. Fabrication of composite films with CNT less than 41 wt % becomes impossible through our technique because the deposited composite film has blocked the passage of the remnant solution through the filtration membrane.

As many works have revealed, superhydrophobicity results from both rough surface structures and low surface free energy.[19−21] Lotus leaves are good examples in nature with their hierarchical surface roughness and a hydrophobic wax coating.[22,23] Pure CNT films prepared by vacuum filtration have rough and porous surface structure (Figure 1c) to

efficiently trap air under the water droplet to separate the liquid−solid phases.[4] A solid Nafion 117 membrane exhibits a strong hydrophobicity with a high contact angle (CA) of 116°.[24] By combining these two elements, CNNFs can realize superhydrophobicity confirmed by wettability measurements. Figure 2b showed two water droplets on the CNNF and the fresh lotus leaf, respectively. The highest CA achieved by CNNF is 165.3 ± 1.9° (Figure 2b, inset). Our investigations also demonstrated that the wettability of the film could be adjusted by varying the chemical composition of the film. We have successfully tuned the chemical composition by both changing the vacuum filtering rate and the content ratio of Nafion to CNT.

The vacuum filtering rate, which determines how fast the solvent of composite solution is pumped through the filtration membrane, is a key factor that affects the surface chemical composition. Figure 2c presents the relationship between the vacuum filtering rates and the water CAs of the respective films. For filtration of the fixed composite solution (35 μL Nafion with 50 mL CNT solution), the water CAs monotonically decrease with increasing the filtering rate. The highest CA up to 165.3 ± 1.9° is achieved at the lowest rate of 0.5 mL/min. When the filtering rate is higher than 2.4 mL/min, a superhydrophobic surface becomes difficult to obtain. During the filtering process, CNTs do not flow through the filtration membrane due to self-aggregation into the interpenetrating network structure, while the Nafion solution could pass through the membrane, leading to Nafion loss with continuous solution flow. As a result, the high filtering rate greatly reduces the amount of Nafion both inside and on the film surface and in turn changes the surface wettability. To confirm that, films were fabricated by different amount of Nafion in the fixed volume of 50 mL CNT solution with a constant filtering rate of 0.5 mL/min and wettability measurements on the films were carried out. The film without Nafion exhibits high water-absorbing property. The water droplets infiltrate the film quickly and completely. Adding as little as 1.4 wt % Nafion content (Figure 2d) dramatically converts the hydrophilic surface into a hydrophobic one (CA = 144.8 ± 5.2°). As the amount of Nafion continues to increase, the surface becomes superhydrophobic and attains the highest CA of 165.3 ± 1.9° at the content ratio of 9.8 wt %. The results are consistent with those obtained by increasing the filtering rate, confirming that the film with lower Nafion content on the surface has a relatively smaller CA. Further increasing Nafion content, however, leads to a decrease of CA and eventually forfeits the superhydrophobicity at 21.0 wt % Nafion content (CA = 149.5 ± 5.9°). The reduction of CA is attributed to the redundant Nafion on the surface, which smoothes the surface roughness.

According to Cassie's Law (eq 1), the relationship between the CA of a water droplet on one component surface (θ) and the CA on a composite surface (θ_C) consisting of air pockets and a solid is described as:[25]

$$\cos\theta_C = f_1\cos\theta - f_2 \quad (1)$$

where f_1 and f_2 represent the areal fractions of solid surface and air pockets touched with liquid, respectively ($f_1 + f_2 = 1$). From the equation, it is clear that the larger the area that the air occupies, the more hydrophobic the composite surface becomes. Therefore, increasing the air trapped at the surface by roughing the surface will increase the CA, while smoothing the surface will decrease the CA. The surface topographies of the CNNFs were examined by SEM. The images revealed the difference in surface roughness of the films with various Nafion contents. On the surface of the film without Nafion (Figure 3a), there are a large number of CNTs densely pressed together but accordingly few pores with the size beyond 100 nm. With the addition of Nafion, the densely packed CNTs gradually loosen up, resulting in the appearance of 100 nm sized pores on the surface of the films made by adding 1.4 wt % and 2.8 wt % Nafion (Figure 3b,c). The pores become deeper and larger with increasing Nafion content, making CNTs detach from each other to form a hierarchical 3D interpenetrating network. However, as Nafion contents are larger than 9.8 wt %, CNTs slowly shrink back (Figure 3e,f) and the pores gradually close up. With the deepest and largest pores formed on the surface of the film with 9.8 wt % Nafion, the CA reaches the highest value (Figure 3d).

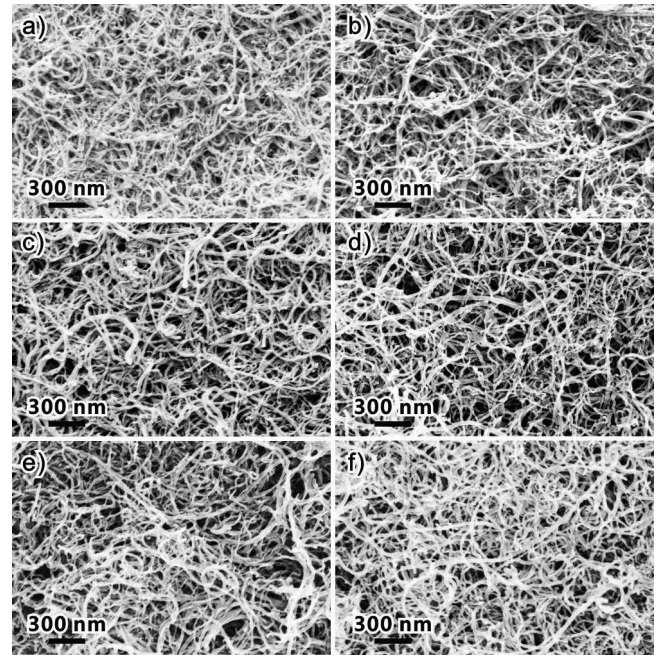

Figure 3. SEM images of CNT films prepared (a) without Nafion, and with Nafion content of (b) 1.4 wt %, (c) 2.8 wt %, (d) 9.8 wt %, (e) 14.0 wt %, and (f) 21.0 wt %.

Unlike observing the surface topology of the single-phase solid surface by SEM, the smart observation of the air−solid−liquid three-phase interface by using the episcopic illumination microscopy (EIM) via a Nikon microscope (eclipse E600 POL), makes air pockets "visible" at the water-repellent interface. The observed images are captured by a digital camera (DXM1200F). As illustrated in Figure 4a, a water droplet of 10 μL is transferred onto the surface of a CNNF preimmobilized on the microscope stage, and the objective is set directly over the water droplet. The focus is adjusted to the interface between the film surface and the water droplet to obtain a clear view. Once the water drop is moved from the viewing field, the view immediately turns blurred, suggesting that the spherical water droplet worked as an extra objective that cooperatively magnified the surface

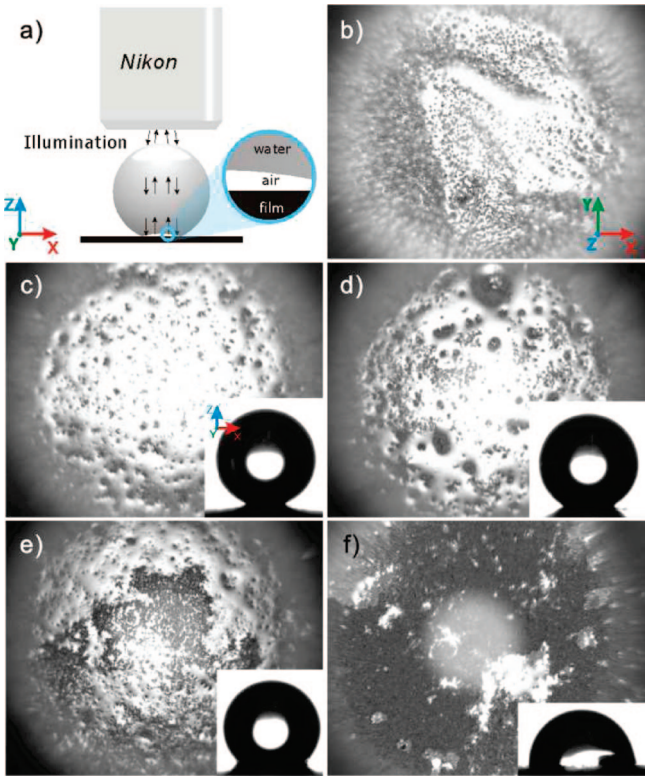

Figure 4. (a) Schematic illustration of the experiment setup of observing the air−solid−liquid three-phase interface by episcopic illumination microscopy. The air−solid−liquid interface of the water droplet (10 μL) on (b) lotus leaf and on CNNFs prepared at the fitering rate of (c) 0.5 mL/min, (d) 2.4 mL/min, (e) 10.0 mL/min, and (f) 16.7 mL/min. The insets in (c−f) show the shapes of water droplet (1 μL) on each CNNFs with contact angles of 165.3 ± 1.9°, 154.2 ± 3.6°, 135.6 ± 7.0°, and 104.6 ± 12.3°, respectively.

beneath and modified the focus of the microscope (Supporting Information). By means of this novel method, we conducted observations to the surfaces of both green fresh lotus leaf and nanocomposite films prepared by different filtering rates as described in Figure 2c. At least five different points were randomly observed in all samples. The clear contrast of darkness and brightness observed from the image of the lotus leaf is indicative of the microscopic structure on the lotus leaf surface together with air cushion sandwiched between the leaf and water (Figure 4b). The dark region is due to the light reflection from the interface between the water droplet and the solid surface, whereas the bright region is due to the light reflection from the interface between the water and the air. To verify that the bright region is the light reflection from the trapped air, we imaged the nonair-trapped surfaces and reduced the trapped air by heat (Supporting Information). The results provide direct proof that the observed white regions are indeed the trapped air pockets. In Figure 4b, it is clearly seen that the bright region occupies the majority of the circular area, showing there is a lot of air trapped under the water droplets. Those tiny dark dots inside the bright region correspond to the papillaes on the surface of lotus leaf.[22,26,27] The same contrast variation patterns are also observed for the nanocompsite films (Figure 4c−f). The more hydrophobic the CNNF, the larger the

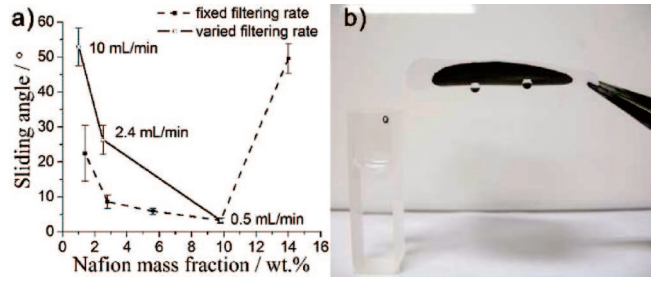

Figure 5. (a) The dependence of the sliding angle of CNNFs on the vacuum filtering rate (solid line) and Nafion content ratio (dotted line). (b) Two drops of water (10 mg) hang upside down on the CNNF (prepared by 21.0 wt % Nafion at 0.5 mL/min filtering rate). The liquid in the colorimetric ware indicates gravity direction.

bright region (more air trapped on the film surface). To the best of our knowledge, the simple yet powerful method we developed gives the first direct observation of the trapped air on a hydrophobic surface.

An ideal superhydrophobic surface should exhibit not only high CA but also low sliding angle (SA). The sliding angle (defined as the difference between advancing and receding contact angle) measurements using 10 mg water droplet give a general understanding of the CA hysteresis for the CNNFs studied above (Figure 5a). The films with high CAs exhibit low SAs, i.e., small CA hysteresis and vice versa. Particularly, the film with the highest CA of 165.3 ± 1.9° has the smallest SA of 3.3 ± 0.7°, and the water droplet can easily roll in all directions on the surface. By comparison, the one prepared at the highest filtering rate (16.7 mL/min) and the one prepared using the most Nafion (21.0 wt%) show high CA hysteresis and can hold the 10 mg water droplet when turned upside down (Figure 5b). Hence, their SAs are not given in Figure 5a. The high adhesive force between the film and the water droplet is believed to result from the enhanced van der Waal's forces between the densely packed CNTs and the water.[28]

The CNNF with high conductivity has been employed as a flexible electrode in an electrochemical biosensor for detecting β-nicotinamide adenine dinucleotide (NADH), which is an important cofactor of dehydrogenases participating in numerous metabolic redox reactions. The electrochemical detection using an ordinary electrode (e.g., glassy carbon) usually confronts the issue of the large overvoltage on NADH oxidation.[29] Many works have been done to develop novel electrode materials that can decrease the overvoltage on NADH oxidation. Figure 6 compares cyclic voltammograms of NADH at glassy carbon (a) and flexible CNNF (b) electrodes. Oxidation at glassy carbon exhibits a high peak potential of +820 mV, while that at CNNF electrode shows a dramatic reduction of the anodic peak potential to +150 mV. The value is even lower than the reported for MWNT-modified glassy carbon (+330 mV).[30] The high catalytic activity toward NADH oxidation accounts for the substantial decrease of 670 mV in anodic peak potential, suggesting that CNNF electrode is a particularly promising candidate for constructing dehydrogenase-based biosensors.

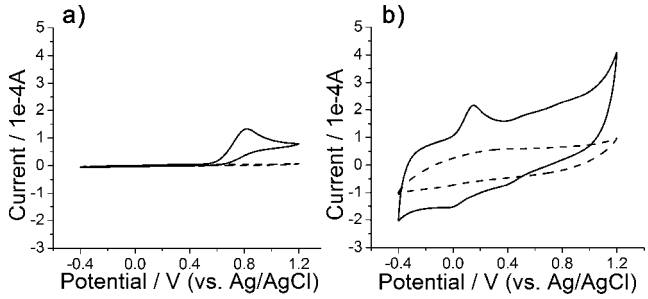

Figure 6. Cyclic voltammograms scanned with 50 mV/s for 12 mM NADH at (a) glassy carbon and (b) flexible CNNF electrodes in a phosphate buffer (50 mM, pH 7.4). Background responses are plotted as dotted lines.

In summary, we successfully fabricated a new flexible multifunctional CNT/Nafion composite film with superhydrophobicity and high conductivity via the vacuum filtering method. The surface wettability of nanocomposite film can be conveniently controlled by varying the filtering rate and the content ratio of Nafion to CNT in the composite solution. The films fabricated by filtering a 9.8 wt % Nafion composite solution with filtering rate of 0.5 mL/min exhibit the highest CA of 165.3 ± 1.9° and the smallest SA of 3.3 ± 0.7°. The fatigue test showed that the films retained the superhydrophobicity and the electric conductivity after 1000 bending cycles. A simple but powerful method has been successfully developed to directly observe the air−solid−liquid three-phase interface using episcopic illumination microscopy for the first time. The dramatic reduction of anodic peak potential by the flexible CNNF electrode in cyclic voltammograms of NADH demonstrates the great potentials of CNNFs in the application of dehydrogenase-based biosensors.

Acknowledgment. This work was financially supported by the 973 Project (2009CB623604, 2009CB930604, 2006CB933000, 2007CB936000) from the Ministry of Science and Technology, National Natural Science Foundation of China (20873175, 20725516) and Shanghai Municipal Commission for Science and Technology (0752nm021).

Supporting Information Available: Description of film preparation method, fatigue tests, electrical conductivity, SEM, water contact angle, EIM, electrochemical measurements, optical path analysis, and verification of the trapped air. This material is available free of charge via the Internet at http://pubs.acs.org.

References

(1) Baughman, R. H.; Zakhidov, A. A.; de Heer, W. A. *Science* **2002**, *297*, 787–792.
(2) Cao, A. Y.; Dickrell, P. L.; Sawyer, W. G.; Ghasemi-Nejhad, M. N.; Ajayan, P. M. *Science* **2005**, *310*, 1307–1310.
(3) Zhang, M.; Fang, S. L.; Zakhidov, A. A.; Lee, S. B.; Aliev, A. E.; Williams, C. D.; Atkinson, K. R.; Baughman, R. H. *Science* **2005**, *309*, 1215–1219.
(4) Wu, Z. C.; Chen, Z. H.; Du, X.; Logan, J. M.; Sippel, J.; Nikolou, M.; Kamaras, K.; Reynolds, J. R.; Tanner, D. B.; Hebard, A. F.; Rinzler, A. G. *Science* **2004**, *305*, 1273–1276.
(5) Lee, K.; Wu, Z.; Chen, Z.; Ren, F.; Pearton, S. J.; Rinzler, A. G. *Nano Lett.* **2004**, *4*, 911–914.
(6) Trancik, J. E.; Barton, S. C.; Hone, J. *Nano Lett.* **2008**, *8*, 982–987.
(7) Ajayan, P. M.; Tour, J. M. *Nature* **2007**, *447*, 1066–1068.
(8) Lau, K. K. S.; Bico, J.; Teo, K. B. K.; Chhowalla, M.; Amaratunga, G. A. J.; Milne, W. I.; McKinley, G. H.; Gleason, K. K. *Nano Lett.* **2003**, *3*, 1701–1705.
(9) Sun, T. L.; Liu, H. A.; Song, W. L.; Wang, X.; Jiang, L.; Li, L.; Zhu, D. B. *Angew. Chem., Int. Ed.* **2004**, *43*, 4663–4666.
(10) Ci, L. J.; Manikoth, S. M.; Li, X. S.; Vajtai, R.; Ajayan, P. M.; Af Ci, L.; Manikoth, S. M.; Li, X.; Vajtai, R.; Ajayan, P. M. *Adv. Mater.* **2007**, *19*, 3300–3303.
(11) Sethi, S.; Ge, L.; Ci, L.; Ajayan, P. M.; Dhinojwala, A. *Nano Lett.* **2008**, *8*, 822–825.
(12) Tasis, D.; Tagmatarchis, N.; Bianco, A.; Prato, M. *Chem. Rev.* **2006**, *106*, 1105–1136.
(13) Wang, J.; Musameh, M.; Lin, Y. *J. Am. Chem. Soc.* **2003**, *125*, 2408–2409.
(14) Ajayan, P. M.; Schadler, L. S.; Giannaris, C.; Rubio, A. *Adv. Mater.* **2000**, *12*, 750–753.
(15) Liu, T. X.; Phang, I. Y.; Shen, L.; Chow, S. Y.; Zhang, W. D. *Macromolecules* **2004**, *37*, 7214–7222.
(16) Bokobza, L. *Polymer* **2007**, *48*, 4907–4920.
(17) Haggenmueller, R.; Gommans, H. H.; Rinzler, A. G.; Fischer, J. E.; Winey, K. I. *Chem. Phys. Lett.* **2000**, *330*, 219–225.
(18) Bin, Y.; Kitanaka, M.; Zhu, D.; Matsuo, M. *Macromolecules* **2003**, *36*, 6213–6219.
(19) Feng, X. J.; Jiang, L. *Adv. Mater.* **2006**, *18*, 3063–3078.
(20) Lafuma, A.; Quéré, D. *Nat. Mater.* **2003**, *2*, 457–460.
(21) Blossey, R. *Nat. Mater.* **2003**, *2*, 301–306.
(22) Feng, L.; Li, S. H.; Li, Y. S.; Li, H. J.; Zhang, L. J.; Zhai, J.; Song, Y. L.; Liu, B. Q.; Jiang, L.; Zhu, D. B. *Adv. Mater.* **2002**, *14*, 1857–1860.
(23) Barthlott, W.; Neinhuis, C. *Planta* **1997**, *202*, 1–8.
(24) Zawodzinski, T. A.; Springer, T. E.; Davey, J.; Jestel, R.; Lopez, C.; Valerio, J.; Gottesfeld, S. *J. Electrochem. Soc.* **1993**, *140*, 1981–1985.
(25) Cassie, A. B. D.; Baxter, S. *Trans. Faraday Soc.* **1944**, *40*, 546–551.
(26) Zhai, J.; Li, H. J.; Li, Y. S.; Li, S. H.; Jiang, L. *Physics* **2002**, *31*, 483–486.
(27) Osawa, S.; Yabe, M.; Miyamura, M.; Mizuno, K. *Polymer* **2006**, *47*, 3711–3714.
(28) Jin, M. H.; Feng, X. J.; Feng, L.; Sun, T. L.; Zhai, J.; Li, T. J.; Jiang, L. *Adv. Mater.* **2005**, *17*, 1977–1981.
(29) Blaedel, W.; Jenkins, R. *Anal. Chem.* **1975**, *47*, 1337–1343.
(30) Musameh, M.; Wang, J.; Merkoci, A.; Lin, Y. H. *Electrochem. Commun.* **2002**, *4*, 743–746.

NL802411D